RESEARCH MEMORANDUM

for the

Bureau of Aeronautics, Department of the Navy

INVESTIGATION OF PERFORMANCE OF AXIAL-FLOW COMPRESSOR OF XT-46 TURBINE-PROPELLER ENGINE

I - PRELIMINARY INVESTIGATION AT 50-, 70-, AND 100-PERCENT DESIGN EQUIVALENT SPEED

By John W. R. Creagh and Donald M. Sandercock

Lewis Flight Propulsion Laboratory
Cleveland, Ohio

NATIONAL ADVISORY COMMITTEE
FOR AERONAUTICS
WASHINGTON

JUNE 13 1950

NATIONAL ADVISORY COMMITTEE FOR AERONAUTICS

RESEARCH MEMORANDUM

for the

Bureau of Aeronautics, Department of the Navy

INVESTIGATION OF PERFORMANCE OF AXIAL-FLOW COMPRESSOR OF XT-46 TURBINE-PROPELLER ENGINE

I - PRELIMINARY INVESTIGATION AT 50-, 70-, and 100-PERCENT DESIGN EQUIVALENT SPEED

By John W. R. Creagh and Donald M. Sandercock

SUMMARY

An investigation is being conducted to determine the performance of the 12-stage axial-flow compressor of the XT-46 turbine-propeller engine. This compressor was designed to produce a pressure ratio of 9 at an adiabatic efficiency of 0.86. The design pressure ratios per stage were considerably greater than any employed in current aircraft gas-turbine engines using this type of compressor.

The compressor performance was evaluated at two stations. The station near the entrance section of the combustors indicated a peak pressure ratio of 6.3 at an adiabatic efficiency of 0.63 for a corrected weight flow of 23.1 pounds per second. The other, located one blade-chord downstream of the last stator row, indicated a peak pressure ratio of 6.97 at an adiabatic efficiency of 0.81 for a corrected weight flow of 30.4 pounds per second. The difference in performance obtained at the two stations is attributed to shock waves in the vicinity of the last stator row. These shock waves and the accompanying flow choking, together with interstage circulatory flows, shift the compressor operating curves into the region where surge would normally occur. The inability of the compressor to meet design pressure ratio is probably due to boundary-layer buildup in the last stages, which cause axial velocities greater than design values that, in turn, adversely affect the angles of attack and turning angles in these blade rows.

INTRODUCTION

The performance of gas-turbine engines can be improved by increasing the stage pressure ratios of the compressor component if the efficiencies are not adversely affected. Performance investigations of axial-flow compressors from current production models of aircraft gas-turbine engines have shown that stage pressure ratios as high as 1.15 with efficiencies in the neighborhood of 0.80 can be obtained (references 1 and 2). Research on cascades of airfoils and single-stage compressors has shown that considerably higher stage pressure ratios are possible with good efficiencies (references 3 and 4).

The compressor from the XT-46 turbine-propeller engine is designed to produce a pressure ratio of 9 in 12 stages at an efficiency of 0.86 and an altitude of 35,000 feet. Because the average design stage pressure ratio of 1.2 for this compressor is considerably higher than any used in current axial-flow types, an investigation of the performance of the compressor was desired in order to determine whether the design conditions could be realized. Data obtained from the investigation might be useful in indicating some of the problems involved in attaining high pressure ratios and might be expected to reveal procedures to follow in solving them.

The present investigation, initiated at the request of the Bureau of Aeronautics, Navy Department, was conducted to determine the performance of the compressor. Owing to the mechanical design of the compressor, installation of extensive interstage instrumentation was extremely difficult and confined the present investigation to over-all performance. An analysis based on static-pressure measurements along the flow path through the compressor is included to indicate the flow characteristics within the unit.

SYMBOLS

The following symbols are used in this report:

M Mach number based on axial velocity

N rotor speed, rpm

P total pressure, in. Hg abs.

p static pressure, in. Hg abs.

W air weight flow, lb/sec

δ ratio of inlet total pressure to standard sea-level pressure

η adiabatic efficiency

θ ratio of inlet stagnation temperature to standard sea-level temperature

Subscripts:

1 compressor inlet

2 compressor outlet

COMPRESSOR

Compressor design. - The axial-flow compressor of the XT-46 turbine-propeller engine was designed to produce a pressure ratio of 9 under the following conditions:

Altitude	35,000 ft
Airplane velocity	400 mph
Rotor speed	11,450 rpm ($N/\sqrt{\theta}$ = 12,700 rpm)
Over-all efficiency	0.863
Air weight flow	9.885 lb/sec ($W\sqrt{\theta}/\delta$ = 30.0)

Inlet guide vanes were provided to reduce the relative velocity at the inlet of the first row of rotor blades, and a row of stationary vanes was installed immediately downstream of the twelfth-stage stator vanes to provide axial velocities at the annular diffuser inlet. The tip diameter of the rotor was 17.000 inches and the hub diameter varied from 9.196 inches at the inlet to 16.192 inches at the outlet. The over-all length of the unit including the inlet housing section and the annular diffuser was approximately 45 inches. Both the rotor and the stator blades were cast alloy steel, hand finished where necessary to obtain correct profiles. A complete description of the mechanical details of the compressor is given in reference 5. A view of the rotor and a half section of the stator are shown in figure 1.

The blade design for both rotor and stator was based on a symmetrical velocity diagram from hub to tip, radial equilibrium at the

entrance to each blade row, and an axial velocity approximately equal to half the rotor speed. The energy addition in each rotor stage was constant from hub to tip. NACA 65-series airfoil sections were used in constructing the blades with the trailing edges thickened slightly to reduce fabrication difficulties. For design operating conditions, the Reynolds number based on blade chord was constant at 250,000 throughout the compressor.

Mechanical problems. - In the design of this compressor, an effort was made to achieve a light-weight unit without sacrificing reliability. To this end, sheet metal was used extensively in constructing the stator housings, the annular diffuser, and the compressor outer housing that served as the connecting structure between the front and rear bearing housings. In order to reduce the axial length of the compressor to a minimum, the design rotor-stator axial clearances were quite small, in some stages as little as 0.028 inch. Owing to the number of unconventional design features of the compressor, such as cast blades on the rotor and general emphasis on light weight, it was decided to submit the unit to a close scrutiny and determine as accurately as possible the probable mechanical performance of several of the more important compressor components before running tests on the assembly.

By suitable adjustments and alterations of the stator-blade bases, the minimum axial clearances of the blade rows were increased about 50 percent. A spin test of the rotor with blades showed that this component was sufficiently strong to withstand the centrifugal forces at design speed. The rotor was subjected to a vibration test and it was found that its critical speed was approximately 1000 rpm below the design speed of the compressor. Calculations also indicated that the twelfth-stage rotor disk was not strong enough to withstand the maximum thrust forces acting on the rotor owing to pressure loading. A static deflection test showed that, for operation under sea-level conditions at the compressor inlet, the rotor would distort sufficiently to seriously damage the compressor blading. The twelfth-stage rotor section was therefore redesigned to increase the natural frequency of the rotor and to provide additional stiffness. A static test of the rotor assembly with this redesigned section showed that the critical speed of the compressor had been increased above the design speed and the deflections due to pressure loading had been reduced to a negligible value.

In adapting the compressor to the test setup, it was necessary to modify the bearing system and the oil-seal system. Thrust bearings capable of handling the thrust of the compressor rotor were

designed to replace the thrust bearing used in the engine assembly where, owing to the counter thrust of the turbine, the net thrust load was considerably smaller. Because the oil seal on the rear compressor bearing had proved unsatisfactory during low-speed operation at the manufacturer's plant, a new system of oil seals was required for this bearing. A thick shell had to be provided for operating the compressor at design inlet conditions in order to reduce the pressure loading on the compressor outer housing. Owing to the still comparatively low values of axial blade-row clearances, indicators were installed to detect any excessive movement of the rotor relative to the stator.

In the first attempt to reach design speed of the compressor, the front air seal failed at approximately 70-percent design speed. Minor damage to the compressor blading resulted and a new air-seal design was required. After a test run of about three hours at design speed, the compressor operation was terminated by the presence of excessive oil leakage in the rear bearing section. The test rig was disassembled and the rear compressor bearing-housing support struts were found to be badly cracked and the oil supply line broken. This part was considered unsafe for further use and a replacement part, considerably stiffened by the addition of extra supporting members, is currently being built and instrumented.

APPARATUS AND PROCEDURE

Apparatus. - Air was supplied to the compressor through a metering orifice and flowed through piping into a large tank installed at the compressor inlet in accordance with the specifications of reference 6. Air was discharged from the compressor into a collector connected to the laboratory exhaust system. Motor driven butterfly valves were used in the inlet and outlet piping to vary the compressor operating conditions. A 3000-horsepower variable-speed electric motor was used in conjunction with a speed increaser to drive the compressor.

Instrumentation. - Standard instrumentation was installed in the tank at the compressor inlet to measure pressures and temperatures according to the method described in reference 6. Because of the size of the tank, the air velocities in it were small and could be neglected. Static-pressure taps were installed in the stator casing upstream and downstream of each stator row (fig. 2). Static-pressure taps were also installed one blade-chord downstream of the thirteenth stator (station 24) according to the method outlined in

reference 6 for determining the compressor discharge total pressure. Wall static-pressure taps were provided along the air-flow path through the annular diffuser on both the inner and outer walls. Total pressure in the annular diffuser was measured by means of two rakes, each consisting of five separate probes arranged to measure the pressures in the centers of equal areas. Total temperatures were measured by two rakes, each consisting of five thermocouple probes arranged in a similar manner. These rakes were located in a position corresponding approximately to the entrance section of the combustors (station 29). The compressor instrumentation is given in the following table:

Station (fig. 2)	Static-pressure taps per station		Total-pressure probes per station	Total-temperature probes per station
	Inner wall	Outer wall		
1 - 23	0	1	0	0
24	4	4	0	0
25	1	1	0	0
26	1	1	0	0
27	1	1	0	0
28	1	1	0	0
29	3	3	10	10
30	1	1	0	0

The air flow was measured by a commercial adjustable orifice in conjunction with a water manometer. Inlet, outlet, and compressor-stage pressures were measured by a bank of mercury manometers. Air temperatures were determined by a potentiometer in conjunction with a precision galvanometer.

Procedure. - The compressor was operated at 50-, 70-, and 100-percent design equivalent rotor speed $N/\sqrt{\theta}$. Refrigerated air was used for all the runs in order to reduce the actual rotor speed and to simulate the design altitude conditions. The following table shows the inlet conditions at which the compressor was operated:

Design equivalent speed (percent)	Inlet pressure (in. Hg abs.)	Inlet temperature ($^{\circ}$F)
50	Varied	-10
70	17	-45
100	9	-56

No attempt was made to reach a surge condition for the lowest speed investigated but the air flow was varied from a maximum to surge at each of the higher speeds. The amount of data obtained at design speed was limited by the failure of the rear compressor-bearing housing.

RESULTS

Over-all performance. - The over-all performance characteristics of the compressor are presented in figure 3. The total-pressure ratios shown in figure 3(a) were determined in two ways. One set of curves represents the compressor performance based on measured total pressures at station 29 and is hereinafter called method A. The other set of curves represents the performance based on total pressures calculated from the static pressures measured at station 24 in accordance with the method described in reference 6 and is hereinafter called method B. Total-pressure ratios obtained by each of these methods were used to calculate the adiabatic efficiency and resulted in the two sets of efficiency curves shown in figure 3(b).

A peak pressure ratio of 6.3 determined by method A was obtained at design speed for a corrected weight flow of 23.1 pounds per second. The efficiency at this point, determined by the same method, was 0.63. A peak efficiency of 0.65 was obtained by method A at a corrected weight flow of 26.2 pounds per second. The design equivalent weight flow of 30.0 pounds per second was obtained but at a low value of efficiency and pressure ratio as determined by method A.

Using total pressures calculated according to method B, a maximum total-pressure ratio of 6.97 was obtained at an adiabatic efficiency of 0.81 and a corrected weight flow of 30.4 pounds per second. The performance curves determined by the two methods are fairly close over the lower weight-flow range of the curves. Differences in the curves in this region are probably due to neglect of boundary layer and possible tangential components of velocity at station 24 in calculating the discharge total pressure according to method B. As the flow increased to a maximum value at each speed, however, a sharp divergence in the curves calculated by the two methods can be seen. The probable reasons for this discrepancy are discussed later.

Static-pressure distribution. - The static-pressure distribution along the air-flow path through the compressor is shown in figure 4 for three values of corrected weight flow at design equivalent speed.

The design variation of static pressure is also included in the figure. The experimental static-pressure ratios are somewhat higher than the design curve up to about station 20. Some of the difference between the experimental and design curves may be attributed to the fact that the experimental data were obtained from pressure taps on the outer wall of the compressor, whereas the design values represent an average static pressure from hub to tip. This effect would be most prominent in the first stages where the hub-tip ratios are smallest and would be expected to decrease in the later stages. The divergence of the experimental and design curves in the first few stages is believed to be due to greater-than-design loading in the first-stage rotor and stator, which causes the blade rows up to about station 11 to operate at angles of attack greater than design and, consequently, at static-pressure ratios higher than design. Between stations 11 and 17, the experimental and design curves are nearly parallel, probably because the boundary-layer buildup tends to increase the axial velocities and to decrease the angle of attack and the pressure ratio. Downstream of station 17, the boundary-layer effect becomes predominant and the detrimental effects of poor angles of attack are carried into the following blade rows.

A large drop in static pressure was obtained at station 24 for the maximum corrected weight flow. This drop became smaller as the weight flow decreased and, at the lowest weight flow, a slight pressure rise was obtained. Some pressure recovery was obtained in the annular diffuser (stations 25 through 30) at each of the corrected weight flows. It is evident, however, that serious losses in pressure are occurring across the twelfth and thirteenth stators and that the flow is choking in this region.

Performance at station 24. - Because of the large pressure losses previously mentioned, the flow conditions at station 24 were studied; the results are shown in figure 5 where the Mach number of the flow at station 24 is plotted against corrected weight flow for each of the three compressor speeds. It was assumed in this calculation that no rotational velocity was present and, consequently, the Mach numbers are conservative. For each of the speeds shown, Mach numbers exceeding 1.0 were obtained. Evidently, supersonic velocities exist at this station at the maximum-flow points and it is significant that the highest Mach numbers correspond to the points on figure 3 that exhibit the greatest divergence in pressure ratio and efficiency as determined by methods A and B.

DISCUSSION

The existence of the large drop in static pressure between stations 23 and 24 and the attendant high Mach numbers at station 24 indicate the presence of supersonic velocities and shock waves. Shock waves offer a possible explanation of the discrepancies previously noted in the curves of figure 3. The position of the shock wave for the highest corrected weight flow at each speed is probably somewhere between stations 24 and 25 and moves upstream beyond station 24 as the increases in back pressure are accompanied by decreases in corrected weight flow. At these maximum weight flows, therefore, the measured total pressure at station 29 will be considerably less than the calculated total pressure at station 24 owing to losses across the shock wave. As the shock wave passes upstream beyond station 24, the total pressures determined by methods A and B should be in close agreement inasmuch as no large losses in total pressure are occurring between these two stations.

In view of the existence of the shock waves, it seems probable that in the high corrected-weight-flow region at each speed the performance curves calculated by method B represent the true potential performance of the compressor. As the weight flow is decreased and the shock waves move upstream, the total pressures determined by either method are probably not indicative of the actual compressor performance because of the losses through the shock waves. These losses should not be important at the lowest weight flows, however, where the shock waves would be considerably weaker if not completely absent.

An indication of the compressor performance up to the twelfth-stage stator inlet is shown in figure 6 for design speed where the total-pressure ratio calculated at station 23 is plotted against the corrected weight flow. The curves are for total pressures calculated for no rotational component of air velocity and for an arbitrary rotation equal to one-half the rotor speed. The actual compressor operating characteristic is probably somewhere between the two curves. The peak-pressure-ratio point has shifted to slightly lower weight flows but the curves are quite flat near the peak points. The curves indicate that the compressor was operating in a region of corrected weight flows that would normally be the surge region if the large losses at the compressor outlet were not present. It is believed that surge-free operation was obtained in this region because these losses tended to produce a stable operating curve and because of circulation among the stages due to openings around the bases of the stator blades resulting from the method used to attach

these blades to the stator shell. Communication spaces between the area around the outside of the stator shell and the annular diffuser discharge further complicated the circulating-flow condition.

Although the data presented herein are somewhat limited, sufficient information is available to indicate that the maximum potentialities of the compressor are not being reached. The performance of the first eight stages appears to be good but falls of in the later stages, probably because of boundary-layer buildup and resultant increases in axial velocity. The larger axial velocities alter the flow from the design values, and the degenerative effect is cumulative as the air progresses beyond the ninth stage. The compressor chokes somewhere between stations 23 and 25 at a corrected weight flow approximating the peak-pressure-ratio point. A range of weight flows is obtained by virtue of the interstage circulatory flow, and the large pressure losses that tend to forestall the occurrence of surging and transfer the surge point to lower flows. Removing the twelfth and thirteenth stator rows would probably result in an increase in weight flow due to elimination of the flow-restricting characteristics of these blade rows. Elimination of the interstage leakage paths would remove the losses associated with this circulatory type of flow. Not much increase in total-pressure ratio can be expected with the present compressor configuration, however, unless some changes are made in blade settings in the last few rows. Since no provisions were made to allow blade-angle adjustment, a completely new set of blading would be required. Removal of the boundary layer at the ninth-stage stator might improve the performance by opening up the flow area at this point to obtain a closer approach to design conditions in the succeeding stages. The high axial velocities in this section of the compressor are believed to be the cause of the poor performance inasmuch as the angle of attack on the blades and the turning angle in the blade rows cannot be equal to the design values.

SUMMARY OF RESULTS

From the investigation of the 12-stage axial-flow compressor of the XT-46 turbine-propeller engine, the following results were obtained:

1. Based on performance at a point corresponding to the combustor inlet, a peak pressure ratio of 6.3 was obtained at an adiabatic efficiency of 0.63 and a corrected weight flow of 23.1 pounds per second.

2. Based on performance at a station one blade-chord downstream of the thirteenth stator, a peak pressure ratio of 6.97 was obtained at an adiabatic efficiency of 0.81 and a corrected weight flow of 30.4 pounds per second.

3. Shock waves occurring in the vicinity of the thirteenth stator row are believed to account for the discrepancy in values of total pressures determined at the two stations in the compressor discharge. At the high values of corrected weight flows, pressure ratio and efficiency data obtained for the station one blade-chord downstream of the thirteenth stator row are believed to be more representative of the true compressor performance than the same parameters determined at the simulated combustor entrance.

4. Boundary-layer buildup in the last few stages of the compressor probably accounts for the inability of the compressor to produce the design pressure ratio. The high velocities resulting from this reduction in area adversely affect the angle of attack and turning angle in these stages.

5. Large pressure losses at the compressor discharge combined with interstage circulatory flows permit the compressor to operate in the flow region where surge would normally occur.

Lewis Flight Propulsion Laboratory,
National Advisory Committee for Aeronautics,
Cleveland, Ohio, May 10, 1950.

John W. R. Creagh
John W. R. Creagh,
Aeronautical Research Scientist.

Donald Sandercock
Donald Sandercock,
Aeronautical Research Scientist.

Approved: Robert O. Bullock
Robert O. Bullock,
Aeronautical Research Scientist.

Oscar W. Schey
Oscar W. Schey,
Aeronautical Research Scientist.

aap

REFERENCES

1. Finger, Harold B., Cohen, Leo, and Stewart, Warner L.: Investigation of Stage Performance of X24C-2 Ten-Stage Axial-Flow Compressor at Design Speed. NACA RM SE50E01, 1950.

2. Prince, William R., and Jansen, Emmert T.: Altitude-Wind-Tunnel Investigation of Compressor Performance on J47 Turbojet Engine. NACA RM E9G28, 1949.

3. Bogdonoff, Seymour M., and Bogdonoff, Harriet E.: Blade Design Data for Axial-Flow Fans and Compressors. NACA ACR L5F07a, 1945.

4. Burtt, Jack R.: Investigation of Performance of Typical Inlet Stage of Multistage Axial-Flow Compressor. NACA RM E9E13, 1949.

5. Carleton, Wm.: Initial Testing of the XT-46 Basic Gas Generator. Rep. R-1093, Ranger Aircraft Engines Div., Fairchild Eng. and Airplane Corp., Aug. 3, 1948.

6. NACA Subcommittee on Compressors: Standard Procedures for Rating and Testing Multistage Axial-Flow Compressors. NACA TN 1138, 1946.

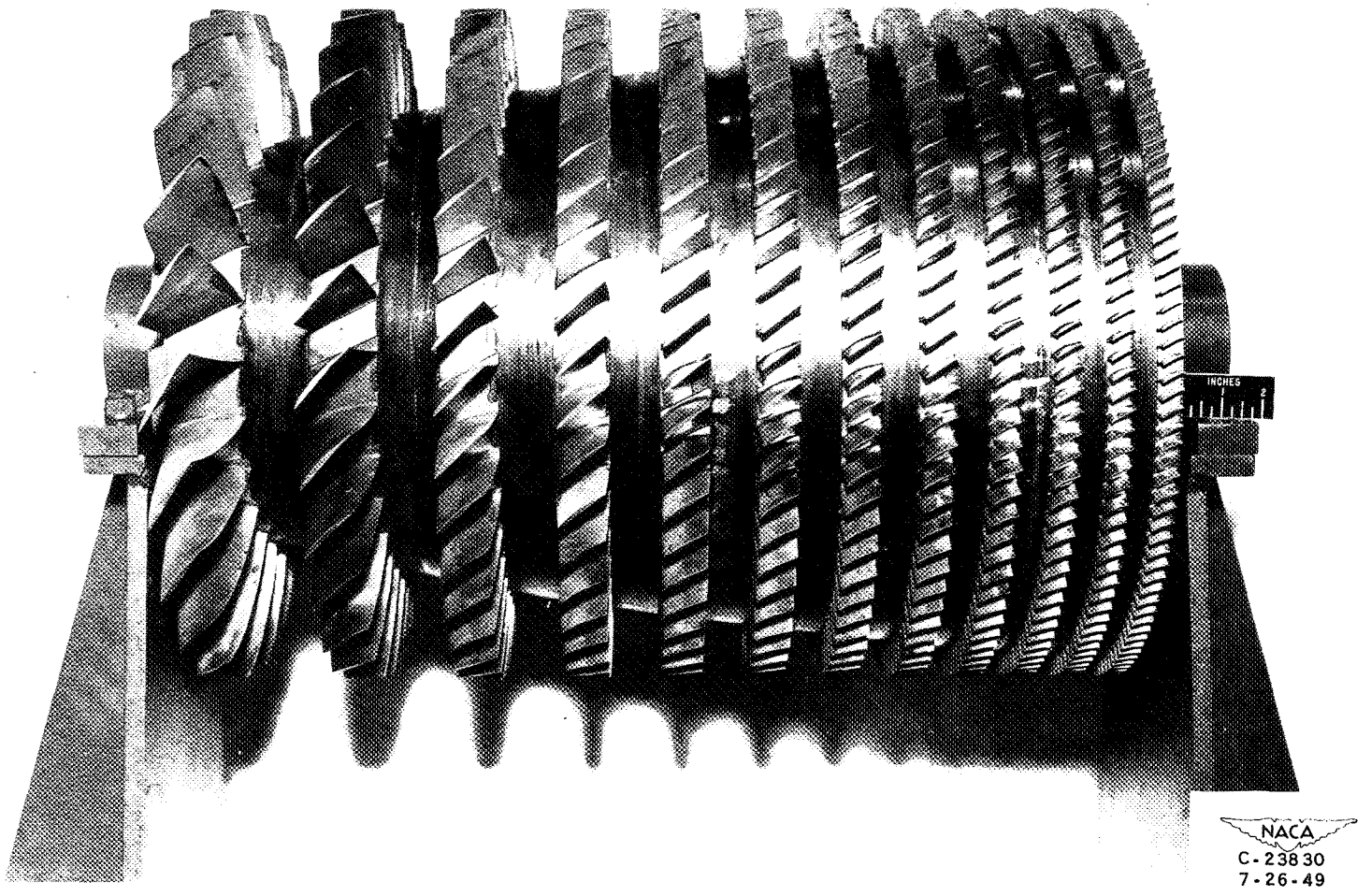

(a) Rotor.

Figure 1. - Components of 12-stage axial-flow compressor of XT-46 turbine-propeller engine.

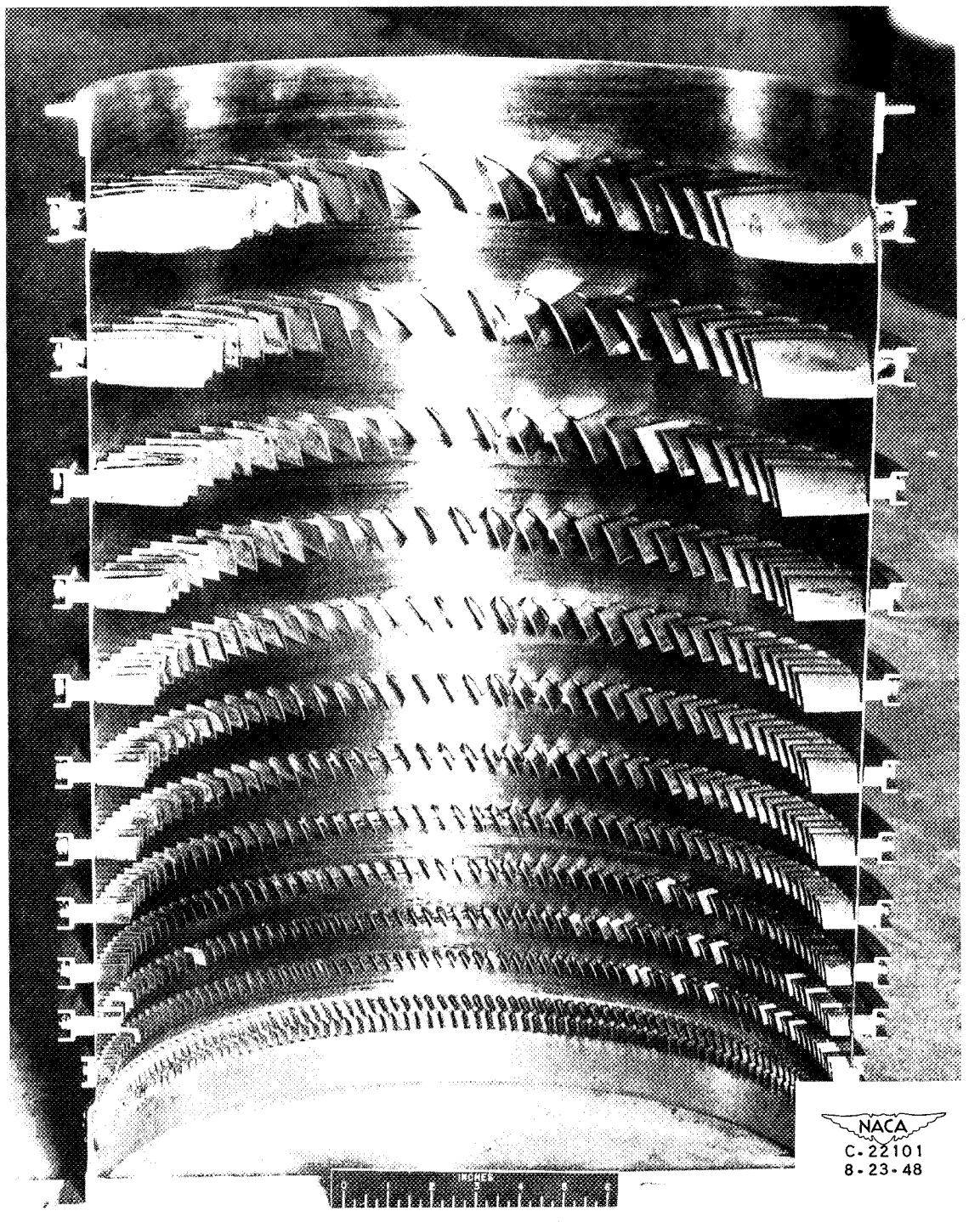

(b) Upper half of compressor casing showing stator blades.

Figure 1. - Concluded. Components of 12-stage axial-flow compressor of XT-46 turbine-propeller engine.

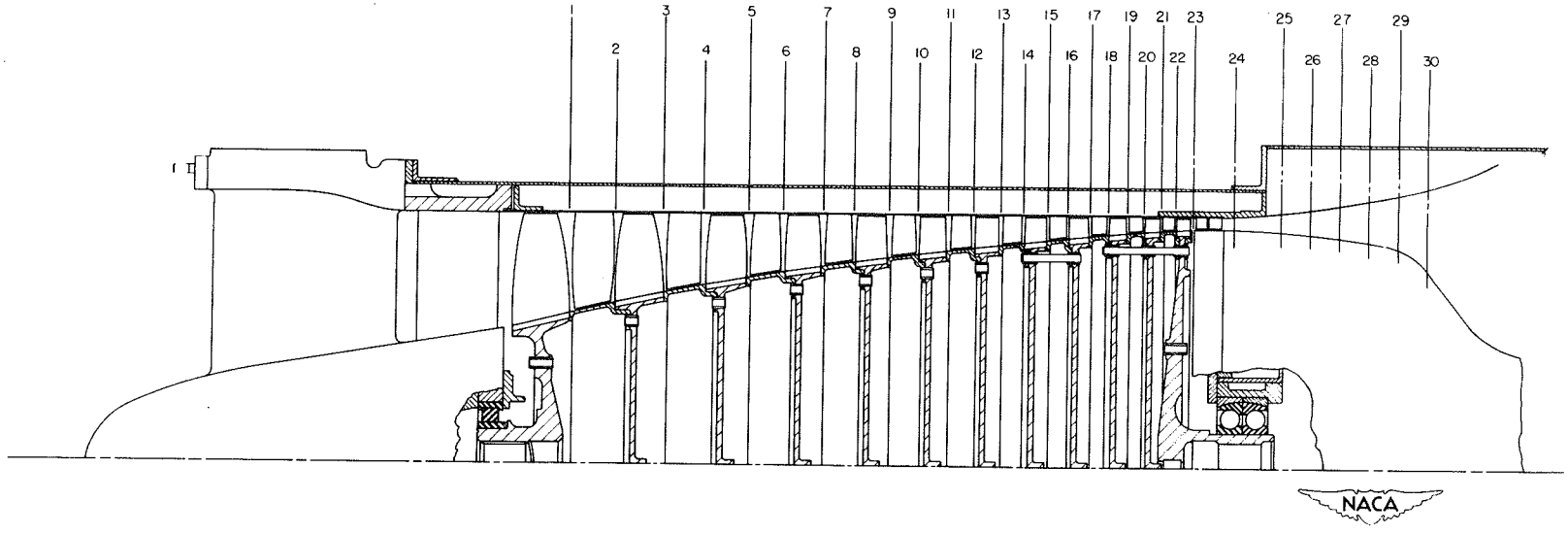

Figure 2. - Half-section of compressor showing measuring-station locations.

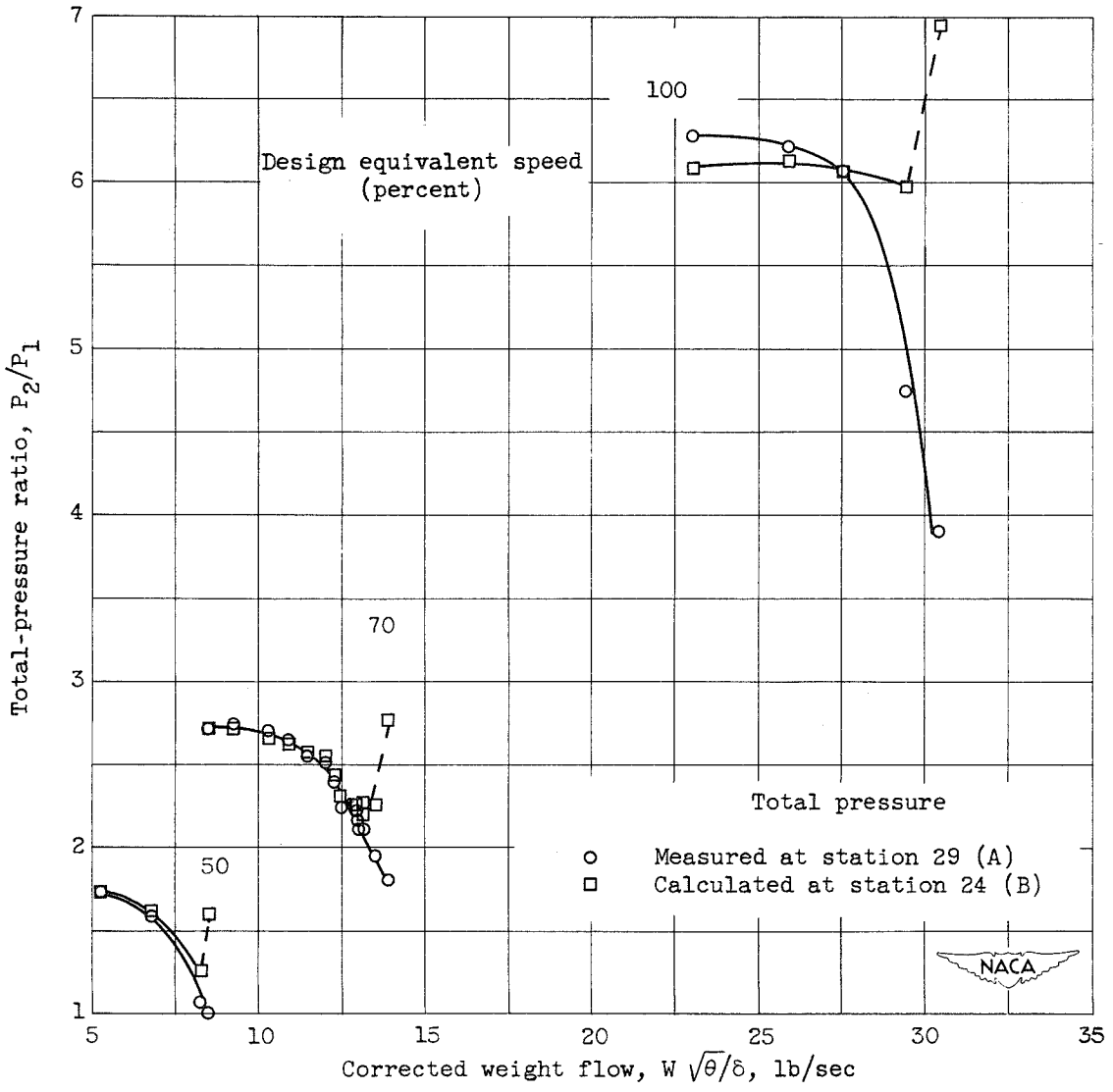

(a) Total-pressure ratio.

Figure 3. - Over-all performance characteristics of axial-flow compressor of XT-46 turbine-propeller engine.

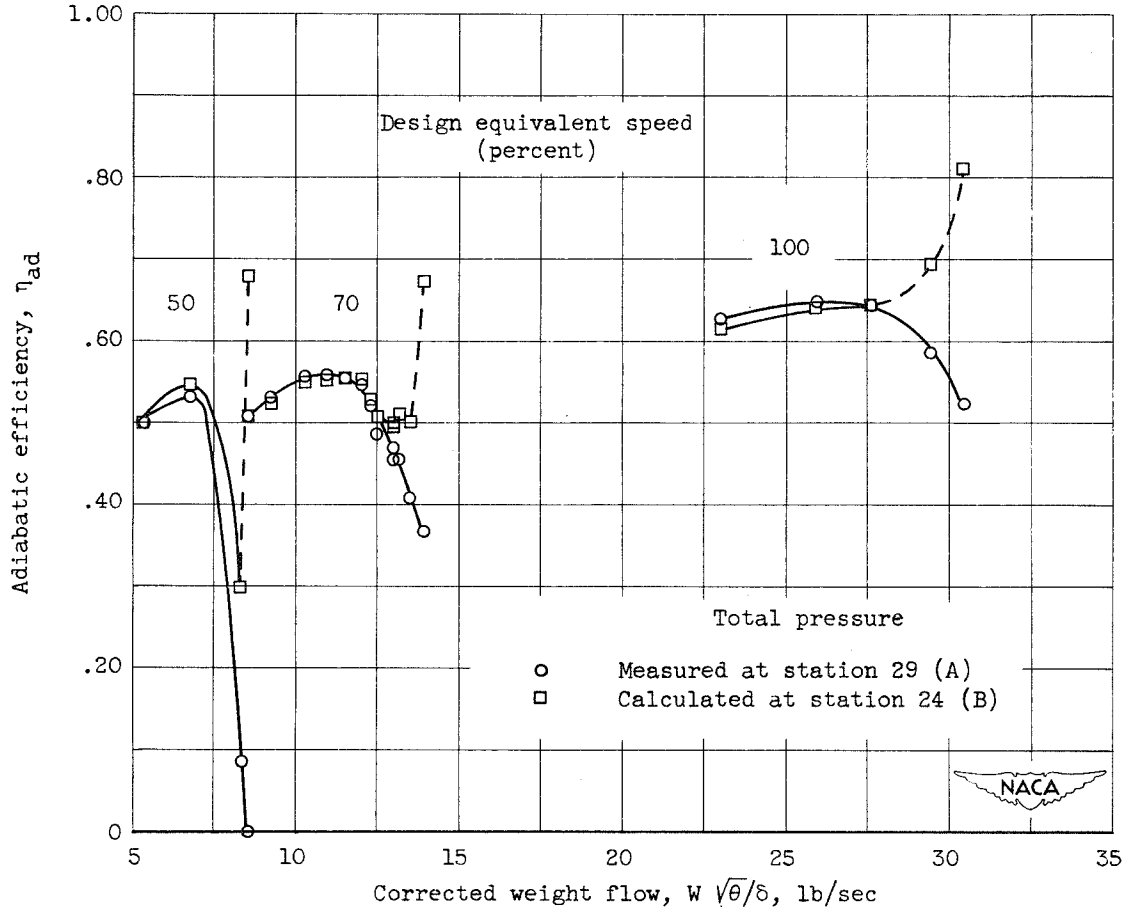

(b) Adiabatic efficiency.

Figure 3. - Concluded. Over-all performance characteristics of axial-flow compressor of XT-46 turbine-propeller engine.

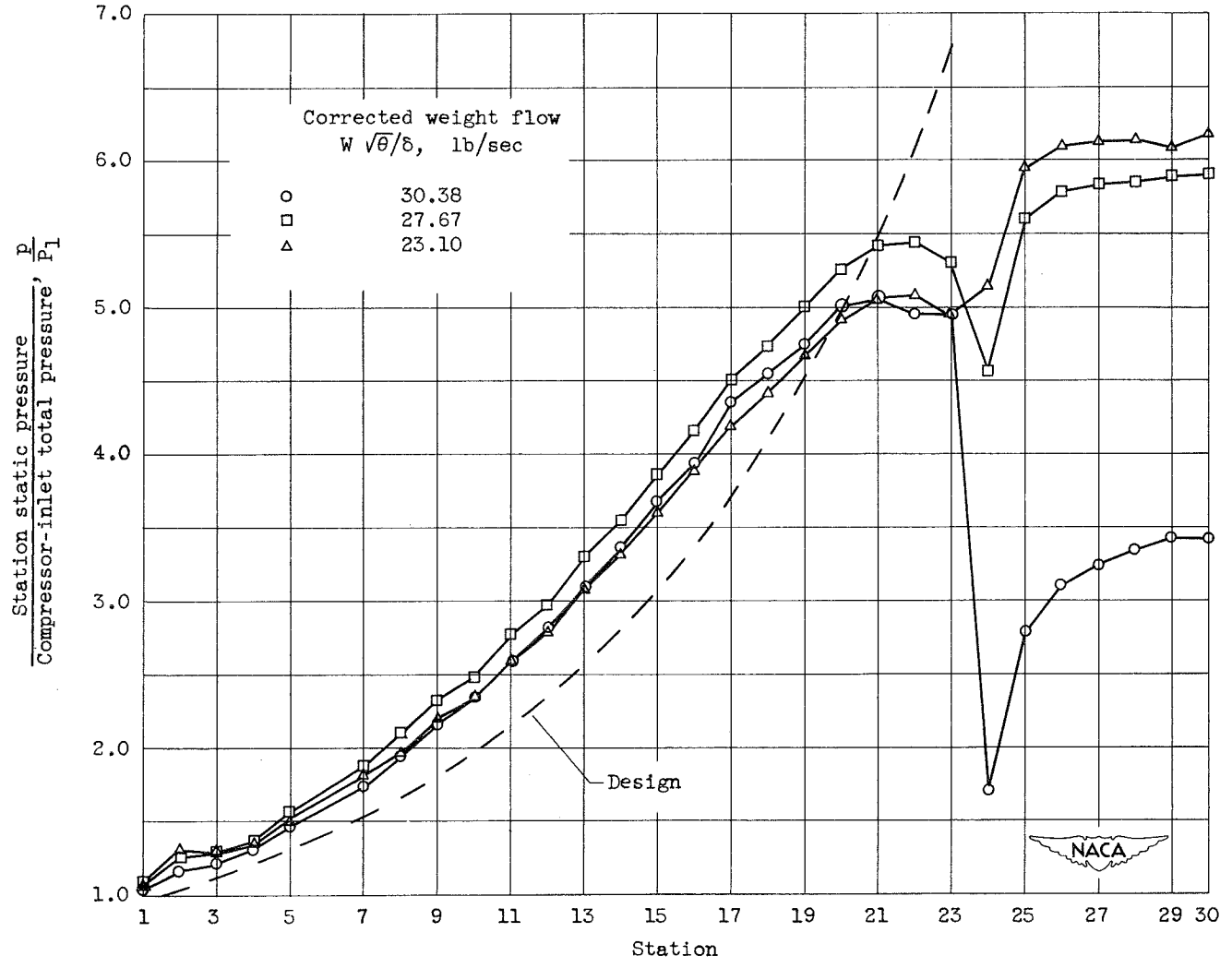

Figure 4. - Static-pressure distribution through 12-stage axial-flow compressor at design equivalent speed.

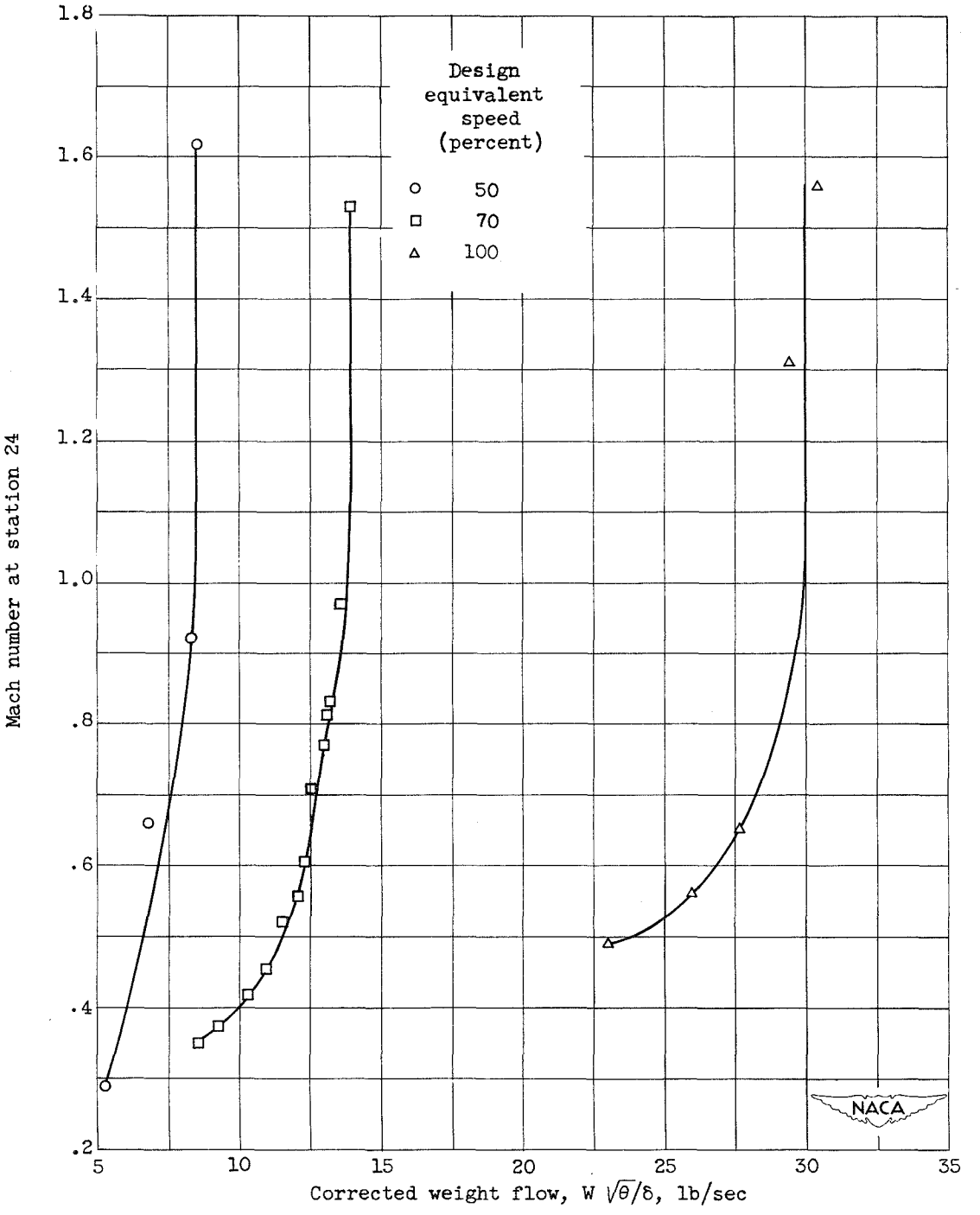

Figure 5. - Mach number at station 24.

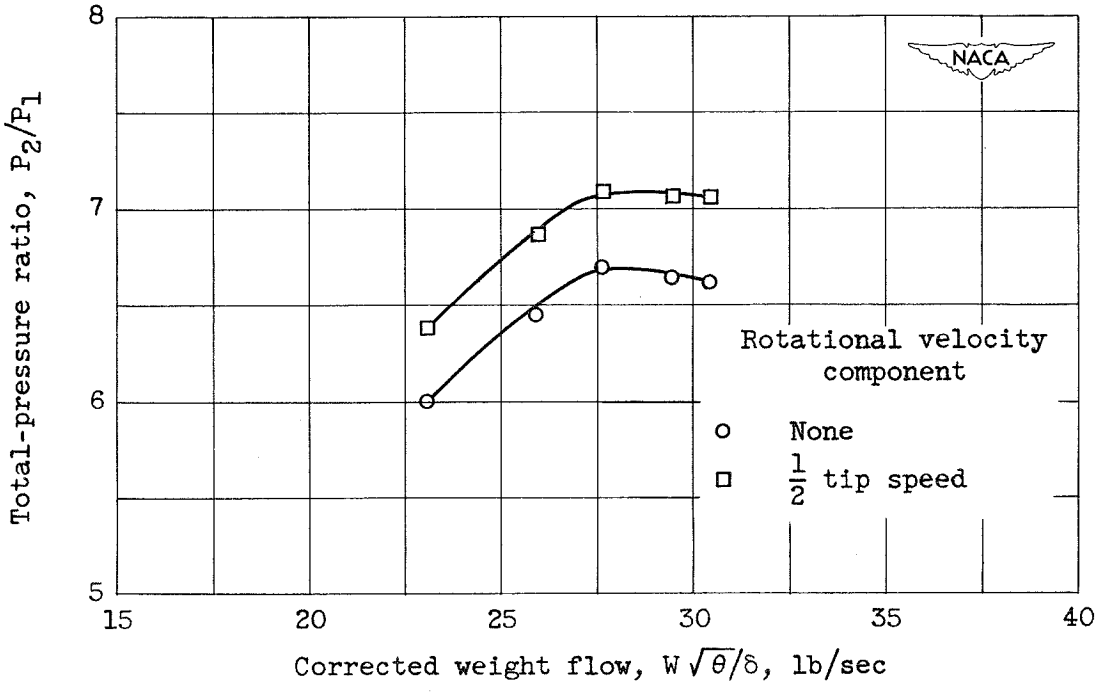

Figure 6. - Variation of total-pressure ratio at twelfth-stage stator inlet with corrected weight flow for two values of rotational velocity.